Title

Moderated Basicity of Endohedral Amine Groups in an Octa-Cationic Self-Assembled Cage

Journal

Angewandte Chemie International Edition, 61(11)

ISSN

1433-7851

Authors

Ngai, Courtney

Wu, Hoi-Ting

Camara, Bryce

et al.

Publication Date

2022-03-07

DOI

10.1002/anie.202117011

Peer reviewed

HHS Public Access

Author manuscript

Angew Chem Int Ed Engl. Author manuscript; available in PMC 2023 March 07.

Published in final edited form as:

Angew Chem Int Ed Engl. 2022 March 07; 61(11): e202117011. doi:10.1002/anie.202117011.

Moderated Basicity of Endohedral Amine Groups in an Octa-Cationic Self-Assembled Cage

Courtney Ngai, **Hoi-Ting Wu**, **Bryce da Camara**, **Christopher G. Williams**, **Leonard J. Mueller**, **Ryan R. Julian**, **Richard J. Hooley***

Department of Chemistry and the UCR Center for Catalysis, University of California - Riverside, Riverside, CA, 92521, U.S.A.

Abstract

A self-assembled $Fe^{II}_4L_6$ cage was synthesized with 12 internal amines in the cavity. The cage forms as the dodeca-ammonium salt, despite the cage carrying an overall 8+ charge at the metal centers, extracting protons from displaced water in the reaction. Despite this, the basicity of the internal amines is lower than their counterparts in free solution. The 12 amines have a sliding scale of basicity, with a ~6 pKa unit difference between the first and last protons to be removed. This moderation of side-chain basicity in an active site is a hallmark of enzymatic catalysis.

Graphical Abstract

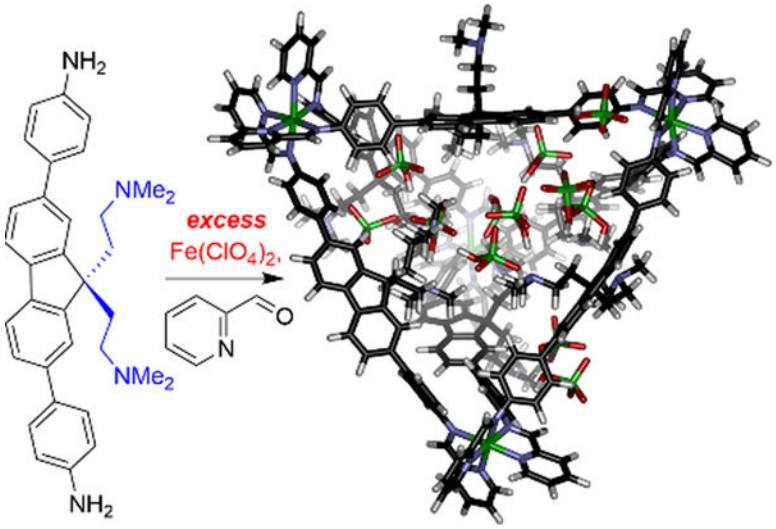

An endohedrally functionalized self-assembled Fe_4L_6 cage complex with 12 internal amines in the cavity acts as an acid host, and shows differential basicity, moderated by the cage superstructure.

Keywords

Supramolecular chemistry; Self-assembly; Coordination Chemistry; Enzyme models; Molecular recognition

*Prof. R. J. Hooley. richard.hooley@ucr.edu.

Enzyme active sites contain sidechain functions that act as acids, and bases to control reactive properties.[1] One of the key facets is that functional group properties in an active site are different than in free solution.[2] For example, in tryptophan synthase, the β-lysine-87 residue adopts different protonation states during the catalysis.[2b] Modulation of sidechain acidity and basicity is key in enzyme mechanism, controlled by the superstructure.[2a]

Synthetic hosts and cages, either organic[3] or metal-organic,[4] are commonly described as "biomimetic".[5] However, the incorporation of reactive functional groups inside biomimetic cage complexes is still a challenge. Metal-mediated self-assembly has been used to synthesize some nanoscale polyhedra with internally positioned functional groups[6] in large $M_{12}L_{24}$ Pd-pyridyl nanospheres,[7] but also in other assembly types.[8] Examples of such functions are oligopeptides,[9] guanidinium ions,[10] polyols[8b, 11] and ureas,[12] which allow selective anion recognition[8, 12] and acid-base catalysis.[12] We have previously incorporated carboxylic acids[13] inside octa-cationic $Fe^{II}_4L_6$ iminopyridine cage complexes, and illustrated the effects on their acidity[13a] and catalytic properties.[13]

In many cases, the biomimetic properties of internal functional groups are explained by simple increases in effective concentration, especially for all-organic neutral scaffolds.[14] Metal-ligand cages are often charged, however, and this charge is an important factor. The effects of cage superstructure on recognition and catalysis have been extensively investigated for *unfunctionalized* highly charged cages (notably by Raymond,[15] Fujita[16] and Ward[17]), but the effect of the charged superstructure on the reactivity of internalized groups is generally underexplored. Here we ask - what is the effect of a charged superstructure on internalized functional groups? To answer this, we describe the synthesis of a $Fe^{II}_4L_6$ tetrahedral cage (**1**, Figure 1) that contains 12 internally oriented alkylamine groups, and discuss the effect of the superstructure on their acid-base properties.

Internalizing functions in a self-assembled cage is simplest with a V-shaped ligand such as the 2,7-dianilinofluorenyl scaffold shown in Figure 1.[13] This scaffold has been used to form cages **2** and **3**,[13a] which can bind neutral organic guests and catalyze acid-mediated processes in solution. While the cationic superstructure in **3** can be implicated in its enhanced acidity, cage **3** is a challenging species to analyze, due to its high reactivity and fragility. As such, we aimed to form a cage with basic functions on the interior. Amine-containing ligand **L1** was targeted, as the $-CH_2CH_2NMe_2$ groups should not compete with iminopyridine formation. After some optimization, reaction of 2-dimethylaminoethyl chloride•HCl with 2,7-dibromofluorene and KOH under air-free conditions proved successful. Extension of the core *via* Suzuki coupling with Boc-4-aminophenyl boronic acid[13a] followed by deprotection gave ligand **L1**. With a suitable ligand in hand, attempts were made to perform cage assembly. Usually, basic groups are poorly tolerated: iminopyridine units are transiminated by primary amines,[18] and 2°/3° amines can competitively coordinate structural metals, so there are very few examples of self-assembled metal-ligand cages with appended basic amines.[19] The "standard" procedure that we[13] (and others[8, 20]) use involves heating ligand with $Fe(NTf_2)_2$ and 2-formylpyridine (PyCHO) in acetonitrile in a 3:2:6 ratio. However, these conditions were

unsuccessful with **L1**, giving mainly bis-imine ligand. Using $Fe(ClO_4)_2$ showed some evidence of assembly, and it became clear that only the use of *excess* $Fe(ClO_4)_2$, gave the requisite purple color indicative of Fe-iminopyridine assembly. The optimized conditions (4.65 mM **L1**, 9.3 mM PyCHO, 5.81 mM $Fe(ClO_4)_2$, CH_3CN, 50 °C, 24 h) gave cage **1** in 48% yield after isolation.

The ^1H NMR spectrum of cage **1** is shown in Figure 2a (for full spectral characterization, see Figures S-8 – S-21). The spectrum is complex, but reminiscent of related cages **2** and **3**.[13a] The imine region shows that the resonance for H^e is split into 8 different peaks, corresponding to the three possible isomers, $T/S_4/C_3$.[13a, 20] The estimated isomeric ratio of $T:S_4:C_3$ is ~10:45:45, similar to that shown by **2**.[13a] This assignment is also corroborated by the aniline region for H^f (δ = 5.6 – 6.0 ppm). The initial spectrum, taken in CD_3CN with minimal precautions taken to eliminate water, showed an unexpectedly persistent, broad peak for H_2O. A spectrum taken in glovebox-stored anhydrous CD_3CN allowed a clear view of the internal CH_2 and NMe_2 groups (H^k, H^l and H^m respectively). The cage was characterized further by 2D NMR, including 2D DOSY, which showed all peaks corresponding to a diffusion constant D = 4.04 x 10^{-10} m^2/s. 2D COSY, TOCSY, NOESY, ROESY, DEPT-HSQC and HMBC spectra were acquired (see Supporting Information). The 2D experiments showed some unexpected characteristics. Figure 2b shows expansions of the 2D COSY and 2D ROESY spectra of **1**, and contain clear, unambiguous crosspeaks between the NMe_2 groups (δ ~2.4 – 3.1 ppm, from the different isomeric groups in the three isomers of **1**) and a broad set of mounds between δ ~6.8 – 7.2 ppm. ROESY crosspeaks between the NMe_2 groups and a bound protic guest are unsurprising, but the COSY spectrum shows that the broad groups show *scalar* coupling to the NMe_2 groups as well.

The nature of the internal species was identified by ESI-MS analysis, using an instrument with a nanoESI source and an orbitrap mass analyzer. As can be seen in Figure 2e (see Supporting Information for full spectra and expansions), a series of ions corresponding to protonated forms of cage **1** are seen. Cage **1** is defined here as the $[Fe_4L_6]^{8+}$ assembly, and multiple 8+ ions can be seen with 3–8 accompanying $HClO_4$ species. This explains the broad peaks in the NMR, as the internal NMe_2 groups are *protonated* in solution. The 2D NMR data shows that the internal protons are tightly associated with the NMe_2 groups: the bound protons are persistent for long enough to show both scalar coupling and NOE crosspeaks. Attempts were made to grow X-ray quality crystals of the cage, but were unsuccessful as this is a highly sensitive system. The cartoon representation shown in Figure 2d is most likely the prevailing structure: while the internal amines are “protonated”, the protons are exchangeable (hence the broad peaks in the ^1H NMR), and the cavity occupied with ClO_4^- anions that share the charge. The exact number of ClO_4^- anions is unclear – Figure 2d shows a minimized structure of cage **1** with twelve $HClO_4$ in the cavity, showing that multiple ClO_4^- ions can certainly fit in the interior. The host:guest properties of the cage suggest that the cavity of **1** is blocked, presumably by ClO_4^- ions: when a neutral guest (diethyl 2,2’-(2,7-dibromofluorene)-diacetate,[13a] see Figures S-52–55) was added to the cage, no binding was seen, whereas it shows strong affinity for acid cage **3** (K_a (**3**) = 6.9 ± 1.2 x 10^3 M^{-1}).[13c]

Further experiments were performed to determine how many acids (on average) are present in the solution of **1**. When the sample is treated with D_2O, the crosspeaks in the COSY/ROESY disappear (see Figure S-31), indicating that the protons in proximity to the NMe_2 groups are exchangeable. To remove the protons, cage **1** was carefully titrated with CD_3CN solutions of different bases with varying pKa,[21] from weak bases (N,N-dimethylaniline, pKa (CH_3CN) = 11.4), to intermediate bases (DABCO, pKa (CH_3CN) = 18.3) and strong bases (DBU, pKa (CH_3CN) = 24.3 or KO^{t}Bu, pKa (CH_3CN) = 30). Notably, DABCO was expected to have a very similar basicity to the cage amines (ignoring any cage effects), as its pKa is identical to that of Me_2EtN (18.3[21]). As can be seen in Figure 3, cage **1** is highly tolerant to added base: even after addition of 40 mol.-eq. DABCO, the cage peaks are intact. The reason for the stability of cage to DABCO was immediately obvious (Figure 3b): after 2 equivalents are added, the observed chemical shift DABCO was identical to that of protonated DABCO-H^+ (δ = 3.12 ppm). This shift persisted even after addition of 10 eq. DABCO, indicating that not only is DABCO a far stronger base than the cage amines, but at least 10 protons are present in the cage. While the cage peaks also show shifts in the ^1H NMR, the isomer ratio remains roughly constant, indicating the three isomers behave similarly. The changes in chemical shift were analyzed by a reservoir model (see Supporting Information) to determine the most likely number of protons on the interior. The DABCO-H^+ peak shift is essentially unchanged up to 11 (±1) equivalents, and then falls in a manner that follows a 1:1 deprotonation equilibrium, suggesting that all the amines in **1** are fully protonated. The “first 11” are strong acids (compared to DABCO), and the last is closer in pKa to the added base.

To provide a more accurate picture, the titration was repeated and monitored by UV absorbance spectroscopy, with aliquots of DABCO (from 1 – 40 eq.) added to cage **1** in CH_3CN. The absorbance changes at 320 and 370 nm (Figure 3c, Figure S-32) corroborate the NMR titration results, in that the first set of ammonium ions behave as strong acids, and the final one(s) were closer in acidity to DABCO. Obviously, fitting twelve individual equilibria is impractical, so we fit the datapoints *after* 11 equivalents of base had been added. This assumes that the first 11 H^+ in the cage are strong acids (compared to DABCO), and focuses on the final deprotonation, to determine the pKa of the (**1**•H^+) → **1** reaction. The calculated ΔpK_a (**1**•H^+) was −0.85 ± 0.08, i.e. pKa (**1**•H^+) = 17.4 ± 0.1.

Obviously (**1**•12H^+) is far more acidic than that, and titration with N,N-dimethylaniline provided a “lower limit” for the basicity: in this case, minimal protonation of the amines was seen ($\Delta\delta$ (NMe_2) = 0.07 ppm after addition of 1 mol.-eq. DMA). The stronger bases were less suitable for this analysis: addition of up to 3 mol.-eq. of the DBU or KO^{t}Bu was possible (Figures S-34, 35), but further additions of base above 3 mol.-eq. caused decomposition, indicating that sequestration of the Fe^{II} centers was occurring.

The outcome of this unusual structural arrangement is that the amine cage **1** is *acidic*, and can catalyze the solvolysis of $PhCH(OMe)_2$. This occurs with 5% cage **3** and 6 eq. water with an initial rate of 41 x 10^4 mM/min at 50 °C. This is substantially slower than the equivalent reaction catalyzed by acid cage **3** (2410 x 10^4 mM/min at 23 °C),[13a] but illustrates the acidic reactivity of the ostensibly “basic” cage **1**, reminiscent of the reactivity profile of polyammonium macrocycles.[22] The cage is also capable of inhibiting base-

catalyzed processes. When 5% cage **1** is added to a 5%-DABCO-catalyzed Knoevenagel reaction between malononitrile and benzaldehyde in CD_3CN, no reaction is observed at all after 24h at 23 °C (Figure S-37), whereas in the absence of cage, 75% conversion occurs.

Finally, the relative acidity of the 12 protonated amines in cage **1** was illustrated by reaction with a series of tritylated amines. 12 mol.-eq. tritylated isoquinoline **4** was added to a solution of cage **1** in CD_3CN and a small amount of water, and the reaction monitored by ^1H NMR: this amount of cage should contain enough protons to fully detritylate **4**. The products formed are the *ammonium salt* **5**•H^+ (and triphenylmethanol) – even though a strongly basic amine is formed, no cage decomposition is seen (see Figure S-39), as the product is far more basic than the cage. As can be seen in Figure 4, the initial reaction was extremely rapid, with 20% conversion in ~3 min. However, after the first 3–4 H^+ are removed from the cage, the overall charge lessens, as does the acidity. The reaction slows down rapidly, reaching 40 % conversion after 4h and only 45% after 24 h. After ~1/2 of the protons are removed, the (**1**•$6H^+$) cage is no longer sufficiently acidic enough to promote reaction. This process can be repeated with N-tritylbenzylamine (green line, Figure 4), and follows much the same reaction profile as **4** with no cage decomposition, despite the reaction producing benzylamine, as the $BnNH_2$ product is fully protonated. In contrast, if N-trityl-4-bromoaniline is used (see Figures S-43, 44), the product cannot be protonated by (**1**•xH^+), the neutral aniline is formed, and over time, the cage is transiminated and destroyed. As such, the cage can protect itself against destruction by strong amines, but not weak ones.

Overall, the synthesis and properties of cage **1** are quite unusual. The only way that the cage can be synthesized effectively is in the presence of *excess* $Fe(ClO_4)_2$. Even though only ligand **L1** and 2-formylpyridine are otherwise present in the anhydrous reaction, the amines in the product are fully protonated. Evidently, the protons come from the water formed upon iminopyridine formation, and the resulting “hydroxide” is removed as iron oxide salts, hence the need for excess iron. Interestingly, if the reaction is performed in the presence of activated molecular sieves, **1**•$12H^+$ is still formed, albeit less effectively than in their absence: the cage is an effective water trap. Attempts to replicate this effect using 0.66 eq. $Fe(ClO_4)_2$ and 0.66 eq. $HClO_4$ only gave bis-imine ligand and no cage, suggesting that the multicomponent assembly process is delicately balanced, and addition of strong acid is not helpful. Other Fe^{II} salts were tested: $Fe(NTf_2)_2$, $Fe(OTf)_2$ or $FeSO_4$ yielded either no cage or an unstable assembly. $Fe(BF_4)_2$•$6H_2O$ was an effective surrogate for $Fe(ClO_4)_2$, however, yielding a cage with similar NMR spectra to the ClO_4^- equivalent (Figures S-22, 23). This is to be expected, as we have previously shown that ClO_4^- and BF_4^- act similarly as templates in the formation of Fe_4L_6 tetrahedra with internal H-bond donors.[23]

The truly unusual observation is that this proton trapping occurs in a cationic cage environment: when all 12 amines are protonated, the **1**•$12H^+$ cage carries an overall charge of 20^+. Even if 12 ClO_4^- anions are in close proximity to the amines to moderate the charge, the 2D COSY data shows that the protons are interacting strongly enough with the amines to allow scalar coupling, so some positive charge must reside on the nitrogen centers. Despite the fact that the acid-trapping is required for assembly, the basicity of the internal amines is significantly *lower* than expected (as compared to a small molecule equivalent

in free solution). The 12 ammoniums display a “sliding scale” of acidity, whereby the “first” NMe_2H^+ ions can be removed by N,N’-dimethylaniline (pKa = 11.4). As protons are removed from the cage (and the overall charge lowers from 20^+ towards 8^+), the protons become correspondingly more difficult to remove, and the final proton shows a pKa of 17.4. This is still a full pKa unit less than expected: the cationic superstructure of the cage makes internalized amines less basic than they should be in free solution. This moderation of side-chain basicity, by networked interactions in a controlled active site, is a hallmark of enzymatic catalysis, and illustrates the biomimetic potential of this synthetic system.

Supplementary Material

Refer to Web version on PubMed Central for supplementary material.

Acknowledgments

The authors would like to thank the National Science Foundation (CHE-2002619 to R.J.H., CHE-1904577 to R.R.J.) and the National Institutes of Health (GM097569 to L.J.M.) for support.

References

[1]. a)Walsh C, Enzymatic Reaction Mechanisms; W. H. Freeman, 1979.b)Fersht A, Structure and mechanism in protein science: a guide to enzyme catalysis and protein folding; Macmillan, 1999.

[2]. a)Jencks WP, Catalysis in Chemistry and Enzymology; McGraw-Hill, 1969.b)Caulkins BG, Bastin B, Yang C, Neubauer TJ, Young RP, Hilario E, Huang YM, Chang CA, Fan L, Dunn MF, Marsella MJ, Mueller LJ, J. Am. Chem. Soc 2014, 136, 12824–12827. [PubMed: 25148001]

[3]. a)Hof F, Craig SL, Nuckolls C, Rebek J Jr. Angew. Chem., Int. Ed 2002, 41, 1488–1508.b)Jordan JH, Gibb BC, Chem. Soc. Rev 2015, 44, 547–585. [PubMed: 25088697]

[4]. Ward MD, Raithby PR, Chem. Soc. Rev 2013, 42, 1619–1636. [PubMed: 22797247]

[5]. a)Breslow R, Acc. Chem. Res 1995, 28, 146–153.b)Brown CJ, Toste FD, Bergman RG, Raymond KN, Chem. Rev 2015, 115, 3012–3035. [PubMed: 25898212] c)Kirby AJ, Angew. Chem., Int. Ed. Engl 1996, 35, 707–724.

[6]. Bogie PM, Miller TF, Hooley RJ, Isr. J. Chem 2019, 59, 130–139.

[7]. Suzuki K, Iida J, Sato S, Kawano M, Fujita M, Angew. Chem. Int. Ed 2008, 47, 5780–5782.

[8]. a)Mal P, Schultz D, Beyeh K, Rissanen K, Nitschke JR, Angew. Chem. Int. Ed 2008, 47, 8297–8301.b)Riddell IA, Smulders MMJ, Clegg JK, Nitschke JR, Chem. Commun 2011, 47, 457–459.c)Zhang D, Ronson TK, Mosquera J, Martinez A, Guy L, Nitschke JR, J. Am. Chem. Soc 2017, 139, 6574–6577. [PubMed: 28463507] d)Zhang D, Ronson TK, Mosquera J, Martinez A, Nitschke JR, Angew. Chem. Int. Ed 2018, 57, 3717–3721.

[9]. Suzuki K, Kawano M, Sato S, Fujita M, J. Am. Chem. Soc 2007, 129, 10652–10653. [PubMed: 17685616]

[10]. a)Wang Q-Q, Gonell S, Leenders SHAM, Dürr M, Ivanović-Burmazović I, Reek JNH, Nat. Chem 2016, 8, 225–230. [PubMed: 26892553] b)Gramage-Doria R, Hessels J, Leenders SHAM, Tröppner O, Dürr M, Ivanović-Burmazović I, Reek JNH, Angew. Chem. Int. Ed 2014, 53, 13380–13384.

[11]. Bolliger JL, Belenguer AM, Nitschke JR, Angew. Chem. Int. Ed, 2013, 52, 7958–7962.

[12]. Custelcean R, Bonnesen PV, Duncan NC, Zhang X, Watson LA, Van Berkel G, Parson WB, Hay BP, J. Am. Chem. Soc 2012, 134, 8525–8534. [PubMed: 22545671]

[13]. a)Holloway LR, Bogie PM, Lyon Y, Ngai C, Miller TF, Julian RR, Hooley RJ, J. Am. Chem. Soc 2018, 140, 8078–8081. [PubMed: 29913069] b)Ngai C, Sanchez-Marsetti CM, Harman WH, Hooley RJ, Angew. Chem. Int. Ed 2020, 59, 23505–23509.c)Ngai C, da Camara B, Woods CZ, Hooley RJ, J. Org. Chem 2021, 86, 12862–12871. [PubMed: 34492175]

[14]. Purse BW, Ballester P, Rebek J Jr. J. Am. Chem. Soc 2003, 125, 14682–14683. [PubMed: 14640624]

[15]. a)Hong CM, Bergman RG, Raymond KN, Acc. Chem. Res 2018, 51, 2447–2455. [PubMed: 30272943] b)Fiedler D, Bergman RG, Raymond KN, Angew. Chem., Int. Ed 2004, 43, 6748–6755.c)Pluth MD, Bergman RG, Raymond KN, Science 2007, 316, 85–88. [PubMed: 17412953] d)Hastings CJ, Pluth MD, Bergman RG, Raymond KN, J. Am. Chem. Soc 2010, 132, 6938–6940. [PubMed: 20443566] e)Zhao C, Toste FD, Bergman RG, Raymond KN, J. Am. Chem. Soc 2014, 136, 14409–14412. [PubMed: 25265509]

[16]. a)Yoshizawa M, Tamura M, Fujita M, Science, 2006, 312, 251–254. [PubMed: 16614218] b)Murase T, Nishijima Y, Fujita M, J. Am. Chem. Soc 2012, 134, 162–164. [PubMed: 22145970] c)Takezawa H, Shitozawa K, Fujita M, Nat. Chem 2020, 12, 574–578. [PubMed: 32313238]

[17]. a)Cullen W, Misuraca MC, Hunter CA, Williams NH, Ward MD, Nat. Chem 2016, 8, 231–236. [PubMed: 26892554] b)Cullen W, Metherell AJ, Wragg AB, Taylor CGP, Williams NH, Ward MD, J. Am. Chem. Soc 2018, 140, 2821–2828. [PubMed: 29412665]

[18]. a)Zarra S, Clegg JK, Nitschke JR, Angew. Chem., Int. Ed 2013, 52, 4837–4840.b)Jiménez A, Bilbeisi RA, Ronson TA, Zarra S, Woodhead C, Nitschke JR, Angew. Chem., Int. Ed 2014, 53, 4556–4560.c)McConnell AJ, Aitchison CM, Grommet AB, Nitschke JR, J. Am. Chem. Soc 2017, 139, 6294–6297. [PubMed: 28426930]

[19]. a)Ueda Y, Ito H, Fujita D, Fujita M, J. Am. Chem. Soc 2017, 139, 6090–6093. [PubMed: 28402111] b)Dai F-R, Wang Z, J. Am. Chem. Soc 2012, 134, 8002–8005. [PubMed: 22551401] c)Qiao Y, Zhang L, Li J, Lin W, Wang Z, Angew. Chem. Int. Ed 2016, 55, 12778–12782.

[20]. a)Meng W, Clegg JK, Thoburn JD, Nitschke JR, J. Am. Chem. Soc 2011, 133, 13652–13660. [PubMed: 21790184] b)Ronson TK, Meng W, W.; Nitschke JR, J. Am. Chem. Soc 2017, 139, 9698–9707. [PubMed: 28682628]

[21]. a)Tshepelevitsh S, Kütt A, Lõkov M, Kaljurand I, Saame J, Heering A, Plieger PG, Vianello R, Leito I, Eur. J. Org. Chem 2019, 40 6735–6748.b)Kaljurand I, Kütt A, Sooväli L, Rodima T, Mäemets V, Leito I, Koppel IA, J. Org. Chem 2005, 70, 1019–1028. [PubMed: 15675863]

[22]. Hosseini MW, Lehn J-M, Jones KC, Plute KE, Bowman Mertes K, Mertes MP, J. Am. Chem. Soc 1989, 111, 6330–6335.

[23]. Young MC, Holloway LR, Johnson AM, Hooley RJ, Angew. Chem. Int. Ed 2014, 53, 9832–9836.

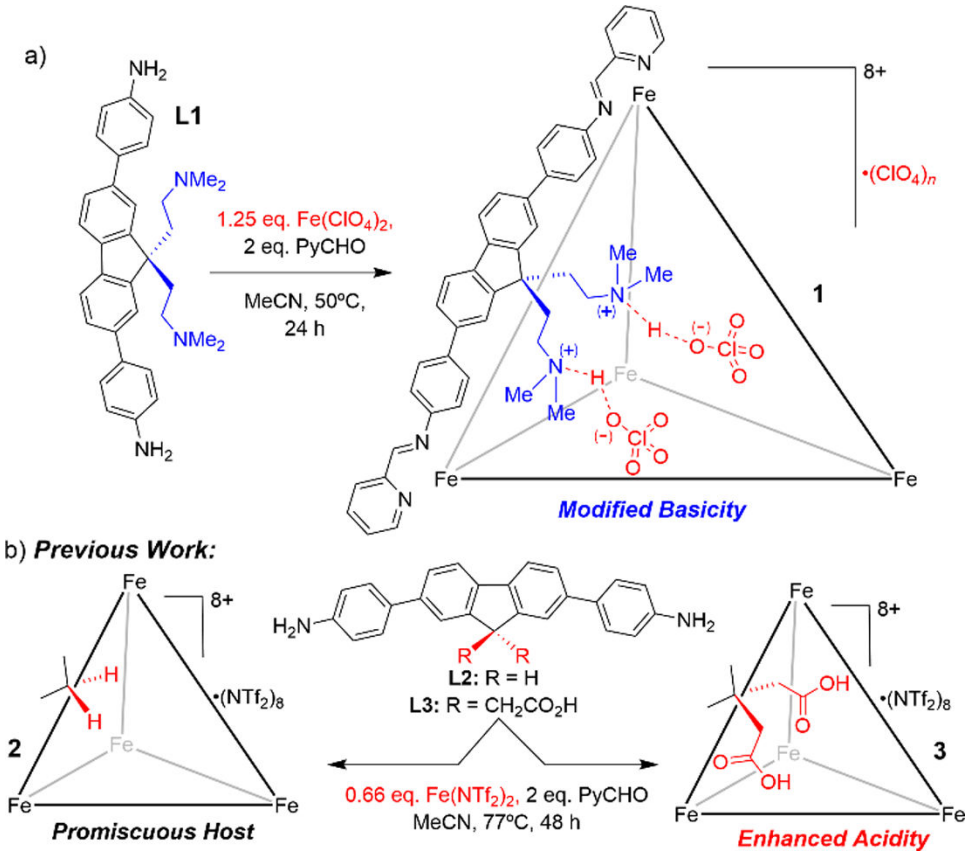

Figure 1.

a) Self-assembly of ligand **L1** into an Fe_4L_6 tetrahedron **1** with internally oriented amine groups and trapped acids. b) Previous Fe_4L_6 tetrahedra from the 2,7-dianilinofluorenyl scaffold.[13a]

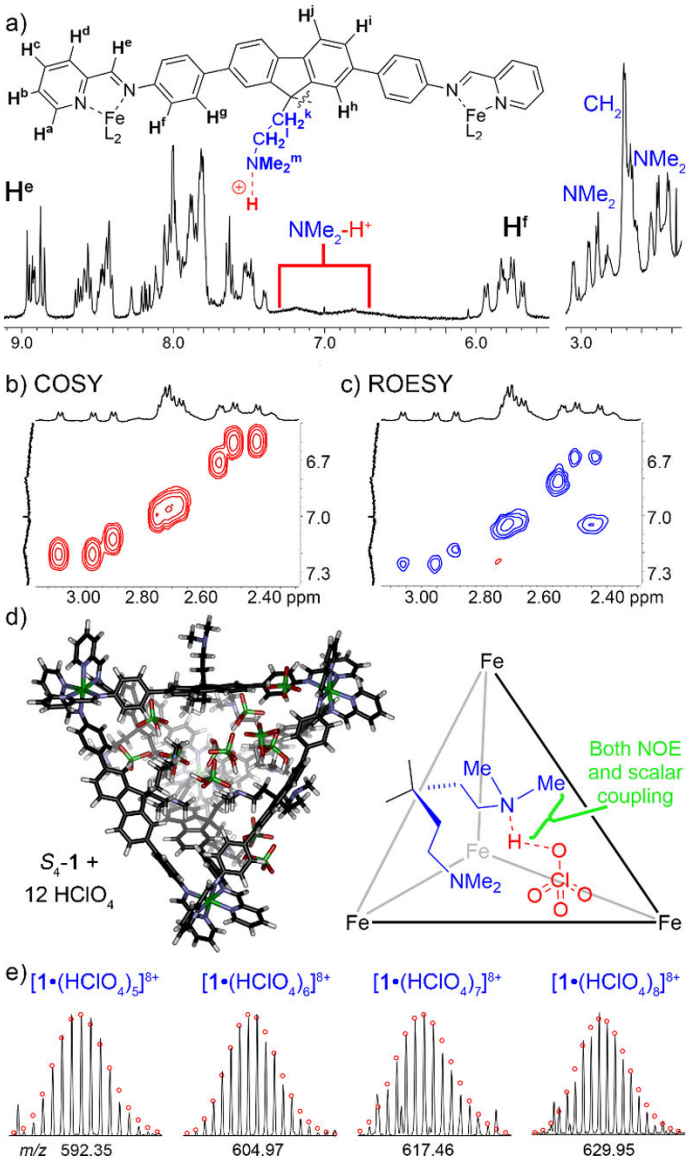

Figure 2.

a) ^{1}H NMR spectrum of **1**; expansions of b) COSY, c) ROESY spectra **(**600 MHz, CD_3CN, 298K, 300 ms mixing time for ROESY); d) minimized structure of S_4-**1** + 12 $HClO_4$; e) peaks observed in the ESI-MS spectrum for 4 different complexes of **1** and $HClO_4$, (red dots indicate theoretical calculated isotope ratio).

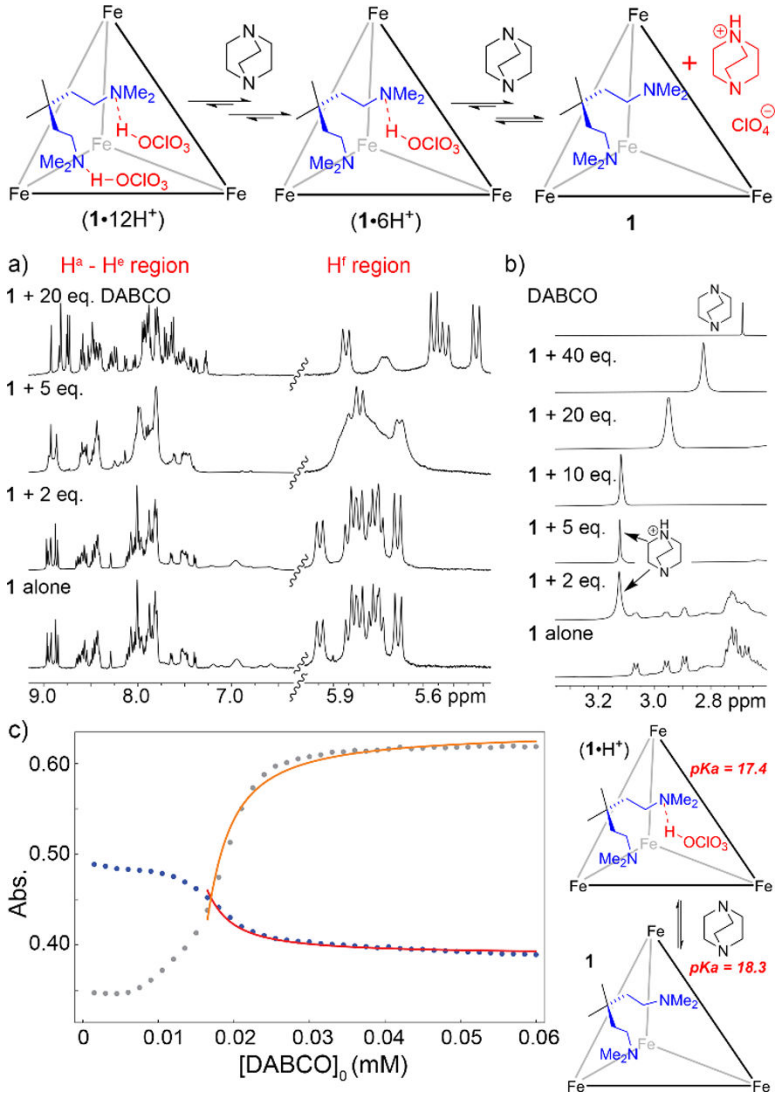

Figure 3.

a) Downfield, and b) upfield regions of the ^{1}H NMR spectra of sequential additions of DABCO to 0.8 mM cage **1** (400 MHz, CD_3CN, 296 K); c) UV absorbance changes of cage **1** (1.5 μM) at 320 nm/370 nm (blue/grey dots) upon titration of DABCO in CH_3CN. Red/yellow lines: fitting trace for the final (**1**•H^+) → **1** equilibrium.

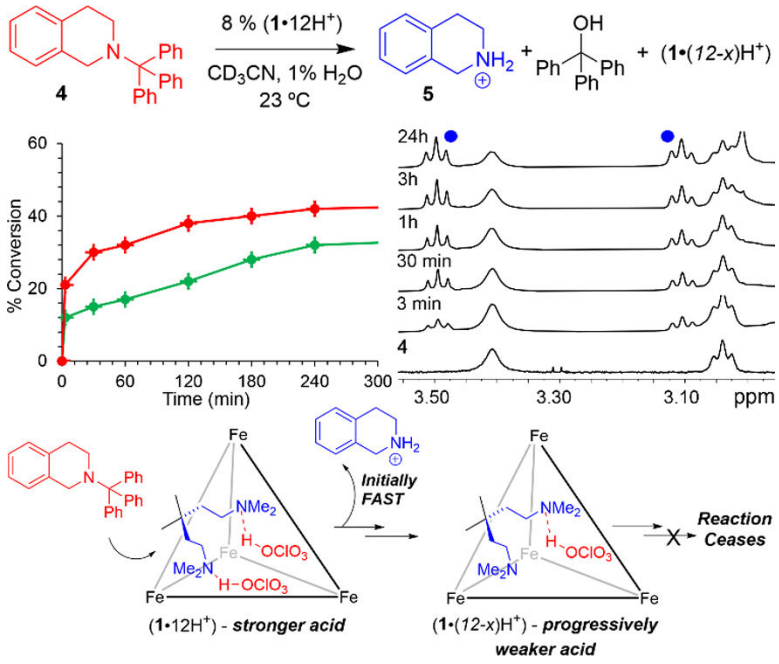

Figure 4.

Amine detritylation promoted by cage **1**. Reaction progress over time monitored by ^{1}H NMR (400 MHz, CD_3CN/1% H_2O, 296 K). [**1**] = 1.25 mM, [**4**] = 15 mM.